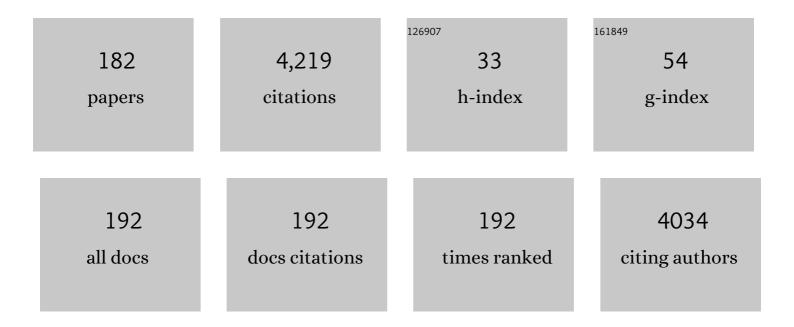
## Yuya Oaki

List of Publications by Year in descending order

Source: https://exaly.com/author-pdf/1143170/publications.pdf Version: 2024-02-01



Υπλα Ολκι

#	Article	IF	CITATIONS
1	Sparse modeling for small data: case studies in controlled synthesis of 2D materials. , 2022, 1, 26-34.		11
2	Electroless nickel plating on a biomineral-based sponge structure. Materials Advances, 2022, 3, 931-936.	5.4	6
3	Performance Predictors for Organic Cathodes of Lithium-Ion Battery. ACS Applied Energy Materials, 2022, 5, 2074-2082.	5.1	8
4	Designed nanostructures created <i>via</i> physicochemical switching of the growth mode between single crystals and mesocrystals. Nanoscale Advances, 2022, 4, 1538-1544.	4.6	1
5	Characterization of calcite spines of planktonic foraminifers (Globigerinidae). CrystEngComm, 2022, 24, 2446-2450.	2.6	1

 $_{6}$  Micro- and nanometric characterization of the celestite skeleton of acantharian species (Radiolaria,) Tj ETQq0 0 0 rg  $_{23}^{BT}$  /Overlock 10 Tf 5

7	A nonclassical pathway to biomimetic strained SrSO <sub>4</sub> crystals. CrystEngComm, 2022, 24, 4356-4360.	2.6	3
8	Nanoarchitectonics for conductive polymers using solid and vapor phases. Nanoscale Advances, 2022, 4, 2773-2781.	4.6	12
9	Ultrastructure of setae of a planktonic diatom, Chaetoceros coarctatus. Scientific Reports, 2022, 12, 7568.	3.3	0
10	A Capacity-Prediction Model for Exploration of Organic Anodes: Discovery of 5-Formylsalicylic Acid as a High-Performance Anode Active Material. ACS Applied Energy Materials, 2022, 5, 8990-8998.	5.1	5
11	Diatom-mimetic channeled mesoporous silica membranes: self-organized formation of a hierarchical porous framework. Materials Chemistry Frontiers, 2021, 5, 862-868.	5.9	1
12	Morphological study of fibrous aragonite in the skeletal framework of a stony coral. CrystEngComm, 2021, 23, 3693-3700.	2.6	7
13	Yield-prediction models for efficient exfoliation of soft layered materials into nanosheets. Chemical Communications, 2021, 57, 5921-5924.	4.1	12
14	Wide-area multilayered self-assembly of fluorapatite nanorods vertically oriented on a substrate as a non-classical crystal growth. Nanoscale, 2021, 13, 9698-9705.	5.6	5
15	Effective 3D open-channel nanostructures of a MgMn <sub>2</sub> O <sub>4</sub> positive electrode for rechargeable Mg batteries operated at room temperature. Journal of Materials Chemistry A, 2021, 9, 6851-6860.	10.3	19
16	Morphological evolution of carbonated hydroxyapatite to faceted nanorods through intermediate states. CrystEngComm, 2021, 23, 2968-2972.	2.6	2
17	Lateral-size control of exfoliated transition-metal–oxide 2D materials by machine learning on small data. Nanoscale, 2021, 13, 3853-3859.	5.6	19
18	Ultrahigh‧ensitive Compression‧tress Sensor Using Integrated Stimuliâ€Responsive Materials. Advanced Materials, 2021, 33, e2008755.	21.0	47

#	Article	IF	CITATIONS
19	Exfoliation Chemistry of Soft Layered Materials toward Tailored 2D Materials. Chemistry Letters, 2021, 50, 305-315.	1.3	19
20	Cellulose intrafibrillar mineralization of biological silica in a rice plant. Scientific Reports, 2021, 11, 7886.	3.3	6
21	Self-Assembly of 2D Nematic and Random Arrays of Sterically Stabilized Nanoscale Rods with and without Evaporation. Langmuir, 2021, 37, 6533-6539.	3.5	2
22	Materials Informatics for 2D Materials Combined with Sparse Modeling and Chemical Perspective: Toward Small-Data-Driven Chemistry and Materials Science. Bulletin of the Chemical Society of Japan, 2021, 94, 2410-2422.	3.2	35
23	A Layered Polydiacetylene Containing Hydrogenâ€Bonding 4,4′â€Bipyridyl Guests: Reversible Color Changes with a Wideâ€Range Temperature Response. ChemPlusChem, 2021, 86, 1563-1568.	2.8	2
24	Sizeâ€Distribution Control of Exfoliated Nanosheets Assisted by Machine Learning: Smallâ€Dataâ€Driven Materials Science Using Sparse Modeling. Advanced Theory and Simulations, 2021, 4, 2100158.	2.8	7
25	Efficient photocatalytic conversion of benzene to phenol on stabilized subnanometer WO <sub>3</sub> quantum dots. Catalysis Science and Technology, 2021, 11, 6537-6542.	4.1	6
26	A Layered Polydiacetylene Containing Hydrogenâ€Bonding 4,4′â€Bipyridyl Guests: Reversible Color Changes with a Wideâ€Range Temperature Response. ChemPlusChem, 2021, 86, 1546.	2.8	1
27	Structured spinel oxide positive electrodes of magnesium rechargeable batteries: High rate performance and high cyclability by interconnected bimodal pores and vanadium oxide coating. Journal of Alloys and Compounds, 2020, 816, 152556.	5.5	26
28	A paper-based device of a specially designed soft layered polymer composite for measurement of weak friction force. Journal of Materials Chemistry C, 2020, 8, 1265-1272.	5.5	24
29	Visualization and Quantification of Microwaves Using Thermoresponsive Color-Change Hydrogel. ACS Sensors, 2020, 5, 133-139.	7.8	28
30	Conjugated Polymers: Solidâ€State Lowâ€Temperature Thermoresponsive and Reversible Color Changes of Conjugated Polymer in Layered Structure: Beyond Infrared Thermography (Small 41/2020). Small, 2020, 16, 2070227.	10.0	3
31	Solidâ€State Lowâ€Temperature Thermoresponsive and Reversible Color Changes of Conjugated Polymer in Layered Structure: Beyond Infrared Thermography. Small, 2020, 16, e2004586.	10.0	12
32	Strained calcite crystals from amorphous calcium carbonate containing an organic molecule. CrystEngComm, 2020, 22, 7054-7058.	2.6	5
33	Intercalation and flexibility chemistries of soft layered materials. Chemical Communications, 2020, 56, 13069-13081.	4.1	25
34	Amorphous flexible covalent organic networks containing redox-active moieties: a noncrystalline approach to the assembly of functional molecules. Chemical Science, 2020, 11, 7003-7008.	7.4	14
35	Efficient Syntheses of 2D Materials from Soft Layered Composites Guided by Yield Prediction Model: Potential of Experimentâ€Oriented Materials Informatics. Advanced Theory and Simulations, 2020, 3, 2000084.	2.8	15
36	Enhancement of coercivity of self-assembled stacking of ferrimagnetic and antiferromagnetic nanocubes. Nanoscale, 2020, 12, 7792-7796.	5.6	9

#	Article	IF	CITATIONS
37	Formation processes, size changes, and properties of nanosheets derived from exfoliation of soft layered inorganic–organic composites. Nanoscale Advances, 2020, 2, 1168-1176.	4.6	11
38	Biomimetic Morphology-Controlled Anhydrous Guanine via an Amorphous Intermediate. Crystal Growth and Design, 2020, 20, 3341-3346.	3.0	9
39	Spinel-Type MgMn <sub>2</sub> O <sub>4</sub> Nanoplates with Vanadate Coating for a Positive Electrode of Magnesium Rechargeable Batteries. Langmuir, 2020, 36, 8537-8542.	3.5	22
40	Thermally induced fragmentation of nanoscale calcite. RSC Advances, 2020, 10, 6088-6091.	3.6	5
41	Guanine crystals regulated by chitin-based honeycomb frameworks for tunable structural colors of sapphirinid copepod, Sapphirina nigromaculata. Scientific Reports, 2020, 10, 2266.	3.3	16
42	Highly porous polymer dendrites of pyrrole derivatives synthesized through rapid oxidative polymerization. Polymer Journal, 2019, 51, 11-18.	2.7	11
43	Amorphous 2D materials containing a conjugated-polymer network. Communications Chemistry, 2019, 2, .	4.5	31
44	Highly Dispersive Mono-sized Nanoparticles of Y <sub>2</sub> O <sub>3</sub> -stabilized ZrO <sub>2</sub> . Chemistry Letters, 2019, 48, 390-393.	1.3	2
45	Experimentâ€Oriented Materials Informatics for Efficient Exploration of Design Strategy and New Compounds for Highâ€Performance Organic Anode. Advanced Theory and Simulations, 2019, 2, 1900130.	2.8	18
46	Glass-transition-induced color-changing resins containing layered polydiacetylene. Chemical Communications, 2019, 55, 11723-11726.	4.1	5
47	Redox-Mediated High-Yield Exfoliation of Layered Composites into Nanosheets. Bulletin of the Chemical Society of Japan, 2019, 92, 779-784.	3.2	21
48	Evolution of Co <sub>3</sub> O <sub>4</sub> Nanocubes through Stepwise Oriented Attachment. Langmuir, 2019, 35, 8025-8030.	3.5	12
49	Quantitative detection of near-infrared (NIR) light using organic layered composites. Journal of Materials Chemistry C, 2019, 7, 4089-4095.	5.5	30
50	Supermicroporous Silica Nanograins: Synthesis and Application. Langmuir, 2019, 35, 5594-5598.	3.5	4
51	Bending Fibers of Hydroxyapatite for Ordered Parallel Architecture in Bovine Tooth Enamel. ACS Omega, 2019, 4, 3739-3744.	3.5	3
52	Enhanced oxide-ion conductivity of solid-state electrolyte mesocrystals. Nanoscale, 2019, 11, 4523-4530.	5.6	7
53	Materialsâ€Informaticsâ€Assisted Highâ€Yield Synthesis of 2D Nanomaterials through Exfoliation. Advanced Theory and Simulations, 2019, 2, 1800180.	2.8	26
54	Artificial mineral films similar to biogenic calcareous shells: oriented calcite nanorods on a self-standing polymer sheet. CrystEngComm, 2018, 20, 1656-1661.	2.6	9

#	Article	IF	CITATIONS
55	Emergence of temperature-dependent and reversible color-changing properties by the stabilization of layered polydiacetylene through intercalation. Polymer Journal, 2018, 50, 319-326.	2.7	21
56	Enhanced electrochemical properties of MgCo2O4 mesocrystals as a positive electrode active material for Mg batteries. Journal of Alloys and Compounds, 2018, 739, 793-798.	5.5	38
57	Layer-by-layer manipulation of anisotropic nanoblocks: orientation-switched superlattices through orthogonal stacking of <i>a</i> and <i>c</i> directions. Nanoscale, 2018, 10, 12957-12962.	5.6	5
58	Nanoscale Mosaic Works: Tetragonal Lattices of Iso-Oriented Heterogeneous Nanocubes. Langmuir, 2018, 34, 4031-4035.	3.5	9
59	Enhanced Quantum Yield of Fluorophores in Confined Spaces of Supermicroporous Silicas. Bulletin of the Chemical Society of Japan, 2018, 91, 87-91.	3.2	12
60	Few-layered titanate nanosheets with large lateral size and surface functionalization: potential for the controlled exfoliation of inorganic–organic layered composites. Chemical Communications, 2018, 54, 244-247.	4.1	23
61	Biomimetic macroscopic mesocrystalline films produced by oriented assembly of nanorods under magnetic field. Nanoscale, 2018, 10, 22161-22165.	5.6	3
62	Crystal-controlled polymerization: recent advances in morphology design and control of organic polymer materials. Journal of Materials Chemistry A, 2018, 6, 23197-23219.	10.3	35
63	Layer-by-Layer Manipulation of Heterogeneous Rectangular Nanoblocks: Brick Work for Multilayered Structures with Specific Heterojunction. Inorganic Chemistry, 2018, 57, 11655-11661.	4.0	14
64	Tunable Stimuliâ€Responsive Colorâ€Change Properties of Layered Organic Composites. Advanced Functional Materials, 2018, 28, 1804906.	14.9	48
65	Multistage redox reactions of conductive-polymer nanostructures with lithium ions: potential for high-performance organic anodes. NPG Asia Materials, 2018, 10, 397-405.	7.9	37
66	Visualization and Quantitative Detection of Friction Force by Selfâ€Organized Organic Layered Composites. Advanced Materials, 2018, 30, e1801121.	21.0	74
67	Two-Dimensional Conductive and Redox-Active Nanostructures Synthesized by Crystal-Controlled Polymerization for Electrochemical Applications. ACS Applied Nano Materials, 2018, 1, 4218-4226.	5.0	9
68	Multistep crystal growth of oriented fluorapatite nanorod arrays for fabrication of enamel-like architectures on a polymer sheet. CrystEngComm, 2017, 19, 669-674.	2.6	21
69	Significant Increase in Band Cap and Emission Efficiency of In <sub>2</sub> O <sub>3</sub> Quantum Dots by Size-Tuning around 1 nm in Supermicroporous Silicas. Langmuir, 2017, 33, 3014-3017.	3.5	24
70	Coupled Exfoliation and Surface Functionalization of Titanate Monolayer for Bandgap Engineering. Advanced Materials Interfaces, 2017, 4, 1601014.	3.7	11
71	Effects of nanostructured biosilica on rice plant mechanics. RSC Advances, 2017, 7, 13065-13071.	3.6	20
72	Bandgap Engineering: Coupled Exfoliation and Surface Functionalization of Titanate Monolayer for Bandgap Engineering (Adv. Mater. Interfaces 7/2017). Advanced Materials Interfaces, 2017, 4, .	3.7	0

#	Article	IF	CITATIONS
73	Phase separation of composite materials through simultaneous polymerization and crystallization. NPG Asia Materials, 2017, 9, e377-e377.	7.9	12
74	Morphology Design of Crystalline and Polymer Materials from Nanoscopic to Macroscopic Scales. Bulletin of the Chemical Society of Japan, 2017, 90, 776-788.	3.2	30
75	Hierarchical bicontinuous structure of redox-active organic composites and their enhanced electrochemical properties. Chemical Communications, 2017, 53, 7329-7332.	4.1	8
76	Real-Time Imaging of 2D and 3D Temperature Distribution: Coating of Metal-Ion-Intercalated Organic Layered Composites with Tunable Stimuli-Responsive Properties. ACS Applied Materials & Interfaces, 2017, 9, 16546-16552.	8.0	39
77	Substrate coating by conductive polymers through spontaneous oxidation and polymerization. Nanoscale, 2017, 9, 7895-7900.	5.6	11
78	Self-Organized Formation of Parallel-Banded Structures through Synchronization of Twisted Growth. Crystal Growth and Design, 2017, 17, 3694-3699.	3.0	3
79	Ultrasensitive Detection of Methylmercaptan Gas Using Layered Manganese Oxide Nanosheets with a Quartz Crystal Microbalance Sensor. Analytical Chemistry, 2017, 89, 12123-12130.	6.5	20
80	Polymer-assisted shapeable synthesis of porous frameworks consisting of silica nanoparticles with mechanical property tuning. Polymer Journal, 2017, 49, 825-830.	2.7	6
81	Tunable Mechano-responsive Color-Change Properties of Organic Layered Material by Intercalation. CheM, 2017, 3, 509-521.	11.7	42
82	Effects of the intercalation rate on the layered crystal structures and stimuli-responsive color-change properties of polydiacetylene. Journal of Materials Chemistry C, 2017, 5, 8250-8255.	5.5	33
83	Spatial Control of Crystallographic Direction in 2D Microarrays of Anisotropic Nanoblocks on Trenched Substrates. Langmuir, 2017, 33, 13805-13810.	3.5	8
84	Hierarchical textures on aragonitic shells of the hyaline radial foraminifer Hoeglundina elegans. CrystEngComm, 2017, 19, 7191-7196.	2.6	5
85	Conductive Polymer Nanosheets Generated from the Crystal Surface of an Organic Oxidant. ChemPlusChem, 2017, 82, 177-180.	2.8	10
86	Two exfoliation approaches for organic layered compounds: hydrophilic and hydrophobic polydiacetylene nanosheets. Chemical Science, 2017, 8, 647-653.	7.4	39
87	Evolution of Calcite Nanocrystals through Oriented Attachment and Fragmentation: Multistep Pathway Involving Bottom-Up and Break-Down Stages. ACS Omega, 2017, 2, 8997-9001.	3.5	12
88	Synthesis of dispersible nanosheets based on monolayer clays with imidazolium and ammonium cations having long-chain alkyl groups. Journal of the Ceramic Society of Japan, 2017, 125, 353-356.	1.1	0
89	Evolution analysis of V <sub>2</sub> O <sub>5</sub> ·nH <sub>2</sub> O gels for preparation of xerogels having a high specific surface area and their replicas. RSC Advances, 2017, 7, 35711-35716.	3.6	12
90	Oriented Attachment of Calcite Nanocrystals: Formation of Single-Crystalline Configurations as 3D Bundles via Lateral Stacking of 1D Chains. Langmuir, 2017, 33, 1516-1520.	3.5	6

#	Article	IF	CITATIONS
91	1D oriented attachment of calcite nanocrystals: formation of single-crystalline rods through collision. RSC Advances, 2016, 6, 61346-61350.	3.6	14
92	Tuning of photocatalytic reduction by conduction band engineering of semiconductor quantum dots with experimental evaluation of the band edge potential. Chemical Communications, 2016, 52, 6185-6188.	4.1	16
93	UV-induced epitaxial attachment of TiO <sub>2</sub> nanocrystals in molecularly mediated 1D and 2D alignments. Chemical Communications, 2016, 52, 7545-7548.	4.1	13
94	Orientation-Selective Alignments of Hydroxyapatite Nanoblocks through Epitaxial Attachment in <i>a</i> and <i>c</i> Directions. Langmuir, 2016, 32, 4066-4070.	3.5	7
95	Tunable photochemical properties of a covalently anchored and spatially confined organic polymer in a layered compound. Nanoscale, 2016, 8, 11076-11083.	5.6	14
96	Incorporation of Redox-active Guest in Conductive and Redox-active Host: Hierarchically Structured Composite of a Conductive Polymer and Quinone Derivative. Chemistry Letters, 2016, 45, 324-326.	1.3	9
97	Mesoscopic crystallographic textures on shells of a hyaline radial foraminifer Ammonia beccarii. CrystEngComm, 2016, 18, 7135-7139.	2.6	21
98	Plant opal-mimetic bunching silica nanoparticles mediated by long-chain polyethyleneimine. RSC Advances, 2016, 6, 1301-1306.	3.6	4
99	Switchable oriented attachment and detachment of calcite nanocrystals. CrystEngComm, 2016, 18, 8999-9002.	2.6	8
100	Evaporation-driven regularization of crystallographically ordered arrangements of truncated nanoblocks: from 1D chains to 2D rhombic superlattices. CrystEngComm, 2016, 18, 6138-6142.	2.6	14
101	Aragonite Nanorod Arrays through Molecular Controlled Growth on Single-Crystalline Substrate and Polysaccharide Surface. Crystal Growth and Design, 2016, 16, 3741-3747.	3.0	11
102	Surface-functionalized hydrophilic monolayer of titanate and its application for dopamine detection. Chemical Communications, 2016, 52, 9466-9469.	4.1	18
103	Intercalationâ€Induced Tunable Stimuliâ€Responsive Colorâ€Change Properties of Crystalline Organic Layered Compound. Advanced Functional Materials, 2016, 26, 3463-3471.	14.9	35
104	Stimuliâ€Responsive Materials: Intercalationâ€Induced Tunable Stimuliâ€Responsive Colorâ€Change Properties of Crystalline Organic Layered Compound (Adv. Funct. Mater. 20/2016). Advanced Functional Materials, 2016, 26, 3462-3462.	14.9	4
105	Orientation-selective alignments of nanoblocks in a and c directions of a tetragonal system through molecularly mediated manipulation. Chemical Communications, 2016, 52, 5597-5600.	4.1	5
106	Morphology and Orientation Control of Organic Crystals in Organic Media through Advanced Biomimetic Approach. Bulletin of the Chemical Society of Japan, 2015, 88, 1459-1465.	3.2	6
107	Inverse pH-response of Temperature-sensitive Copolymers by Combination with Porous CaCO3 Framework. Chemistry Letters, 2015, 44, 1425-1427.	1.3	1
108	Microwave-assisted rapid synthesis of anatase TiO <sub>2</sub> nanosized particles in an ionic liquid-water system. Journal of the Ceramic Society of Japan, 2015, 123, 79-82.	1.1	8

#	Article	IF	CITATIONS
109	Hierarchical CaCO <sub>3</sub> Chromatography: A Stationary Phase Based on Biominerals. Chemistry - A European Journal, 2015, 21, 5034-5040.	3.3	10
110	Hydrophobic monolayered nanoflakes of tungsten oxide: coupled exfoliation and fracture in a nonpolar organic medium. Chemical Communications, 2015, 51, 10046-10049.	4.1	20
111	Surface-functionalized monolayered nanodots of a transition metal oxide and their properties. Physical Chemistry Chemical Physics, 2015, 17, 32498-32504.	2.8	12
112	Polymer-mediated dendritic growth of a transition metal salt crystal as a template for morphogenesis. Polymer Journal, 2015, 47, 183-189.	2.7	12
113	Dynamic adsorption of toluene on pore-size tuned supermicroporous silicas. Microporous and Mesoporous Materials, 2015, 214, 41-44.	4.4	18
114	Fabrication of self-standing films consisting of enamel-like oriented nanorods using artificial peptide. CrystEngComm, 2015, 17, 5551-5555.	2.6	18
115	Controlled radical polymerization of styrene with magnetic iron oxides prepared through hydrothermal, bioinspired, and bacterial processes. RSC Advances, 2015, 5, 51122-51129.	3.6	2
116	Formation of Monocrystalline 1D and 2D Architectures via Epitaxial Attachment: Bottom-Up Routes through Surfactant-Mediated Arrays of Oriented Nanocrystals. Langmuir, 2015, 31, 6197-6201.	3.5	20
117	Fabrication of Transparent ZnO Thick Film with Unusual Orientation by the Chemical Bath Deposition. Crystal Growth and Design, 2015, 15, 3150-3156.	3.0	12
118	Advanced Biomimetic Approach for Crystal Growth in Nonaqueous Media: Morphology and Orientation Control of Pentacosadiynoic Acid and Applications. Chemistry of Materials, 2015, 27, 2627-2632.	6.7	29
119	Crystal-surface-induced simultaneous synthesis and hierarchical morphogenesis of conductive polymers. Chemical Communications, 2015, 51, 9698-9701.	4.1	17
120	A hydrophobic adsorbent based on hierarchical porous polymers derived from morphologies of a biomineral. Chemical Communications, 2015, 51, 7919-7922.	4.1	22
121	Application of biogenic iron phosphate for lithium-ion batteries. RSC Advances, 2015, 5, 68751-68757.	3.6	3
122	Variation in Mesoscopic Textures of Biogenic and Biomimetic Calcite Crystals. Crystal Growth and Design, 2015, 15, 3755-3761.	3.0	7
123	Six-armed twin crystals composed of lithium iron silicate nanoplates and their electrochemical properties. CrystEngComm, 2015, 17, 8486-8491.	2.6	8
124	Formation of uniformly sized metal oxide nanocuboids in the presence of precursor grains in an apolar medium. CrystEngComm, 2015, 17, 7477-7481.	2.6	12
125	VOC decomposition over a wide range of temperatures using thermally stable Cr6+ sites in a porous silica matrix. Catalysis Communications, 2015, 72, 161-164.	3.3	11
126	Incorporation of organic crystals into the interspace of oriented nanocrystals: morphologies and properties. Nanoscale, 2015, 7, 3466-3473.	5.6	10

#	Article	IF	CITATIONS
127	Hydrophobic Inorganic–Organic Composite Nanosheets Based on Monolayers of Transition Metal Oxides. Chemistry of Materials, 2014, 26, 3579-3585.	6.7	52
128	Sizeâ€Dependent Thermochromism through Enhanced Electron–Phonon Coupling in 1 nm Quantum Dots. Angewandte Chemie - International Edition, 2014, 53, 10706-10709.	13.8	18
129	Solvent-free synthesis, coating and morphogenesis of conductive polymer materials through spontaneous generation of activated monomers. Chemical Communications, 2014, 50, 11840-11843.	4.1	21
130	An Experimental Study on the Processes of Hierarchical Morphology Replication by Means of a Mesocrystal: A Case Study of Poly(3,4-ethylenedioxythiophene). Langmuir, 2014, 30, 3236-3242.	3.5	11
131	Basicity-controlled synthesis of Li <sub>4</sub> Ti <sub>5</sub> O <sub>12</sub> nanocrystals by a solvothermal method. RSC Advances, 2014, 4, 44124-44129.	3.6	8
132	Direction Control of Oriented Self-Assembly for 1D, 2D, and 3D Microarrays of Anisotropic Rectangular Nanoblocks. Journal of the American Chemical Society, 2014, 136, 3716-3719.	13.7	77
133	Band-gap expansion of tungsten oxide quantum dots synthesized in sub-nano porous silica. Chemical Communications, 2013, 49, 8477.	4.1	78
134	Microscale pin holders of β-Co(OH)2 and LiCoO2 having a single-crystalline feature. CrystEngComm, 2013, 15, 6465.	2.6	2
135	Formation of <i>c</i> -axis-oriented columnar structures through controlled epitaxial growth of hydroxyapatite. Journal of Asian Ceramic Societies, 2013, 1, 143-148.	2.3	15
136	Monolayered Nanodots of Transition Metal Oxides. Journal of the American Chemical Society, 2013, 135, 4501-4508.	13.7	46
137	Synthesis and Morphogenesis of Organic and Inorganic Polymers by Means of Biominerals and Biomimetic Materials. Chemistry - A European Journal, 2013, 19, 2284-2293.	3.3	20
138	Syntheses of LiCoO <sub>2</sub> Mesocrystals by Topotactic Transformation and Their Electrochemical Properties. ChemPlusChem, 2013, 78, 1379-1383.	2.8	15
139	Thin Films that Consist of CuO Mesocrystal Nanosheets: An Application of Microbialâ€Mineralizationâ€Inspired Approaches to Thinâ€Film Formation. Chemistry - an Asian Journal, 2013, 8, 2064-2069.	3.3	10
140	A Microbialâ€Mineralization Approach for Syntheses of Iron Oxides with a High Specific Surface Area. Chemistry - A European Journal, 2013, 19, 4419-4422.	3.3	11
141	Low-temperature syntheses of cubic BaTiO <sub>3</sub> nanoparticles in highly basic aqueous solution. Journal of the Ceramic Society of Japan, 2013, 121, 388-392.	1.1	4
142	Formation of trigonal microarrays with cubic Ba(NO <sub>3</sub> ) <sub>2</sub> in a polymer matrix. Journal of the Ceramic Society of Japan, 2013, 121, 555-558.	1.1	3
143	A Microbial-Mineralization-Inspired Approach for Systematic Syntheses of Copper Oxides with Controlled Morphologies in an Aqueous Solution at Room Temperature. Bulletin of the Chemical Society of Japan, 2013, 86, 821-828.	3.2	1
144	Self-organization of hollow-cone carbonate crystals through molecular control with an acid organic polymer. Polymer Journal, 2012, 44, 612-619.	2.7	28

#	Article	IF	CITATIONS
145	ZnO nano-rectangular framework-like structure from zinc hydroxide acetate plates. Journal of the Ceramic Society of Japan, 2012, 120, 171-174.	1.1	6
146	Versatile Modification for Highly Dispersive and Functionalized Mesoporous Silica Nanoparticles. Chemistry Letters, 2012, 41, 507-509.	1.3	5
147	Enhanced photoconductive properties of a simple composite coaxial nanostructure of zinc oxide and polypyrrole. Journal of Materials Chemistry, 2012, 22, 21195.	6.7	18
148	Oriented Nanocrystal Mosaic in Monodispersed CaCO <sub>3</sub> Microspheres with Functional Organic Molecules. Crystal Growth and Design, 2012, 12, 876-882.	3.0	46
149	Morphology and orientation control of guanine crystals: a biogenic architecture and its structure mimetics. Journal of Materials Chemistry, 2012, 22, 22686.	6.7	30
150	Mesocrystal nanosheet of rutile TiO <sub>2</sub> and its reaction selectivity as a photocatalyst. CrystEngComm, 2012, 14, 1405-1411.	2.6	53
151	Twisted growth of organic crystal in a polymer matrix: sigmoidal and helical morphologies of pyrene. CrystEngComm, 2012, 14, 7444.	2.6	18
152	Morphological variation of hydroxyapatite grown in aqueous solution based on simulated body fluid. CrystEngComm, 2012, 14, 1143-1149.	2.6	43
153	Crystal-Growth Process of Single-Crystal-like Mesoporous ZnO through a Competitive Reaction in Solution. Crystal Growth and Design, 2012, 12, 2923-2931.	3.0	22
154	Oneâ€Pot Aqueous Solution Syntheses of Iron Oxide Nanostructures with Controlled Crystal Phases through a Microbialâ€Mineralizationâ€Inspired Approach. Chemistry - A European Journal, 2012, 18, 110-116.	3.3	17
155	Homogeneous and Disordered Assembly of Densely Packed Titanium Oxide Nanocrystals: An Approach to Coupled Synthesis and Assembly in Aqueous Solution. Chemistry - A European Journal, 2012, 18, 2825-2831.	3.3	17
156	Synthesis and Morphogenesis of Organic Polymer Materials with Hierarchical Structures in Biominerals. Journal of the American Chemical Society, 2011, 133, 8594-8599.	13.7	49
157	Control of cellular activity of osteoblastic cells with microtopography of biphasic calcium phosphate scaffolds. Journal of the Ceramic Society of Japan, 2011, 119, 635-639.	1.1	2
158	Biomimetic Solidâ€Solution Precursors of Metal Carbonate for Nanostructured Metal Oxides: MnO/Co and MnOâ€CoO Nanostructures and Their Electrochemical Properties. Advanced Functional Materials, 2011, 21, 3673-3680.	14.9	64
159	In Vitro Repair of a Biomineral with a Mesocrystal Structure. Chemistry - A European Journal, 2011, 17, 2828-2832.	3.3	16
160	A Microbialâ€Mineralizationâ€Inspired Approach for Synthesis of Manganese Oxide Nanostructures with Controlled Oxidation States and Morphologies. Advanced Functional Materials, 2010, 20, 4279-4286.	14.9	28
161	Homogeneous and Disordered Assembly of Densely Packed Nanocrystals. Advanced Functional Materials, 2010, 20, 4127-4132.	14.9	14
162	Bioinspired Hierarchical Crystals. MRS Bulletin, 2010, 35, 138-144.	3.5	63

#	Article	IF	CITATIONS
163	Emergence of helical morphologies with crystals: twisted growth under diffusion-limited conditions and chirality control with molecular recognition. CrystEngComm, 2010, 12, 1679.	2.6	39
164	Nanosegregated Amorphous Composites of Calcium Carbonate and an Organic Polymer. Advanced Materials, 2008, 20, 3633-3637.	21.0	119
165	A hierarchical self-similar structure of oriented calcite with association of an agar gel matrix: inheritance of crystal habit from nanoscale. Chemical Communications, 2007, , 2841.	4.1	64
166	Biomimetic morphological design for manganese oxide and cobalt hydroxide nanoflakes with a mosaic interior. Journal of Materials Chemistry, 2007, 17, 316-321.	6.7	38
167	Stereospecific Morphogenesis of Aspartic Acid Helical Crystals through Molecular Recognition. Langmuir, 2007, 23, 5466-5470.	3.5	22
168	Chelationâ€Mediated Aqueous Synthesis of Metal Oxyhydroxide and Oxide Nanostructures: Combination of Ligandâ€Controlled Oxidation and Ligandâ€Cooperative Morphogenesis. Chemistry - A European Journal, 2007, 13, 8564-8571.	3.3	25
169	One-Pot Synthesis of Manganese Oxide Nanosheets in Aqueous Solution: Chelation-Mediated Parallel Control of Reaction and Morphology. Angewandte Chemie - International Edition, 2007, 46, 4951-4955.	13.8	115
170	A Biomimetic Approach for Hierarchically Structured Inorganic Crystals through Self-Organization. Bulletin of the Chemical Society of Japan, 2006, 79, 1834-1851.	3.2	129
171	Nanoengineering in Echinoderms: The Emergence of Morphology from Nanobricks. Small, 2006, 2, 66-70.	10.0	151
172	Preparation of hierarchically organized calcium phosphate–organic polymer composites by calcification of hydrogel. Science and Technology of Advanced Materials, 2006, 7, 219-225.	6.1	63
173	The Hierarchical Architecture of Nacre and Its Mimetic Material. Angewandte Chemie - International Edition, 2005, 44, 6571-6575.	13.8	223
174	Hierarchically organized architecture of potassium hydrogen phthalate and poly(acrylic acid): toward a general strategy for biomimetic crystal design. Chemical Communications, 2005, , 6011.	4.1	47
175	Morphological Evolution of Inorganic Crystal into Zigzag and Helical Architectures with an Exquisite Association of Polymer:Â A Novel Approach for Morphological Complexity. Langmuir, 2005, 21, 863-869.	3.5	58
176	Cover Picture: Emergence of Morphological Chirality from Twinned Crystals (Angew. Chem. Int. Ed.) Tj ETQq0 0 (	) rgBT/Ov 13.8	erlock 10 Tf 5
177	Amplification of Chirality from Molecules into Morphology of Crystals through Molecular Recognition. Journal of the American Chemical Society, 2004, 126, 9271-9275.	13.7	109
178	Experimental Demonstration for the Morphological Evolution of Crystals Grown in Gel Media. Crystal Growth and Design, 2003, 3, 711-716.	3.0	202
179	Layered macrocycles with flexibility and tunable dynamic properties for wide-range thermoresponsive color changes. Sensors & Diagnostics, 0, , .	3.8	5
180	Demonstrated gradual evolution of disorder in crystalline structures between single crystal and	2.6	0

polycrystal <i>via</i> chemical and physicochemical approaches. CrystEngComm, 0, , . 180

#	Article	IF	CITATIONS
181	Water Reduction Photocathodes Based on Ru Complex Dyes Covered with a Conjugated Polymer Nanosheet. Energy & Fuels, 0, , .	5.1	3
182	Preparation of conductive Cu1.5Mn1.5O4 and Mn3O4 spinel mixture powders as positive active materials in rechargeable Mg batteries operative at room temperature. Journal of Sol-Gel Science and Technology, 0, , .	2.4	0